

Electronic entanglement via quantum Hall interferometry in analogy to an optical method

Diego Frustaglia^{1,*} and Adán Cabello^{1,†}

¹*Departamento de Física Aplicada II, Universidad de Sevilla, E-41012 Sevilla, Spain*

(Dated: October 29, 2018)

We present an interferometric scheme producing orbital entanglement in a quantum Hall system upon electron-hole pair emission via tunneling. The proposed setup is an electronic version of the optical interferometer proposed by Cabello *et al.* [Phys. Rev. Lett. **102**, 040401 (2009)], and is feasible with present technology. It requires single-channel propagation and a single primary source. We discuss the creation of entanglement and its detection by the violation of a Bell inequality.

PACS numbers: 03.65.Ud, 03.67.Mn, 73.43.-f 73.23.-b

I. INTRODUCTION

Experimental progress in quantum information requires reliable sources of entanglement. In quantum optics, spontaneous parametric down conversion is a natural source of polarization-entangled photons¹ and can be used to produce energy-time entangled photons after postselection.² These sources and the existence of efficient methods for distributing photons explain the success of quantum optics for long-distance quantum communication.

On the other hand, solid-state nanostructures offer advantages for the local processing of quantum information. This has provoked a major scientific effort towards the development of quantum electronics. Specifically, there is a research program for translating optical technologies which have already proved their applicability for quantum information processing into the realm of quantum electronics. That includes the development of an electronic Mach-Zehnder interferometer,³ several implementations^{4,5} of electronic Hanbury Brown-Twiss interferometers⁶ and, more recently, the proposal⁷ of an electronic Hong-Ou-Mandel interferometer.⁸

In this Rapid Communication we take a further step in this program and present a source of electronic entanglement. This is inspired by a recent photonic interferometer, originally aimed for the production and detection of energy-time and time-bin entanglement,⁹ after noticing that the same scheme can be used to create orbital entanglement by a suitable redefinition of the postselective local measurements. Here, we show that all topological constraints from the optical setup—the basis of its working principle—can be satisfied and the problems derived from fermionic statistics can be overcome by making use of the last developments in quantum Hall physics.⁵ The detection procedure is based on the measurement of zero-frequency current-noise correlators in the tunneling regime. Moreover, the setup presents some distinguishing features over previous proposals requiring either two propagating channels¹⁰ or two sources:^{11,12} it requires, instead, a single channel and a single tunnel barrier as a source of correlated electron-hole pairs.

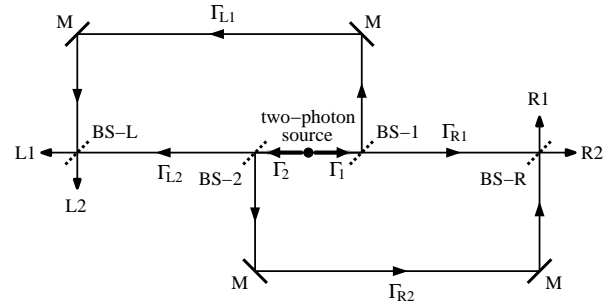


FIG. 1: Optical interferometer introduced in Ref. 9.

II. OPTICAL INTERFEROMETER

We start by reviewing the interferometer introduced in Ref. 9 (see Fig. 1). A source simultaneously emits two photons in opposite directions: photon 1 to the right (along path Γ_1) and photon 2 to the left (along path Γ_2). After meeting beam splitter BS-1 (BS-2), photon 1 (2) splits into a pair of paths Γ_{R1} and Γ_{L1} (Γ_{R2} and Γ_{L2}). Path Γ_{R1} (Γ_{R2}) takes photon 1 (2) to the right side of the interferometer for detection, while path Γ_{L1} (Γ_{L2}) does likewise in the left side.

The complete two-photon state emitted from BS-1 and BS-2 is a coherent superposition of four possible paths combinations represented by kets $|\Gamma_{(L,R)1}, \Gamma_{(L,R)2}\rangle$, with the first site for photon 1 and the second for photon 2. It consists of two contributions in which one photon flies off to the right and the other one to the left ($|\Gamma_{R1}, \Gamma_{L2}\rangle$ and $|\Gamma_{L1}, \Gamma_{R2}\rangle$), and two contributions in which both photons fly off to the same side ($|\Gamma_{R1}, \Gamma_{R2}\rangle$ and $|\Gamma_{L1}, \Gamma_{L2}\rangle$). Photons 1 and 2 are not entangled with each other. However, their state is not separable when rewritten on a left-right bipartition basis, owing both standard mode entanglement (orbital-mode or path entanglement in this case) and occupation-number entanglement (i.e., coherent superposition of terms with different local occupation number).¹³ The orbital entanglement [i.e., the entanglement between left (Γ_{L1}, Γ_{L2}) and right (Γ_{R1}, Γ_{R2}) propagating channels] can be postselected from the total state by coincidence measurements at both sides of the inter-

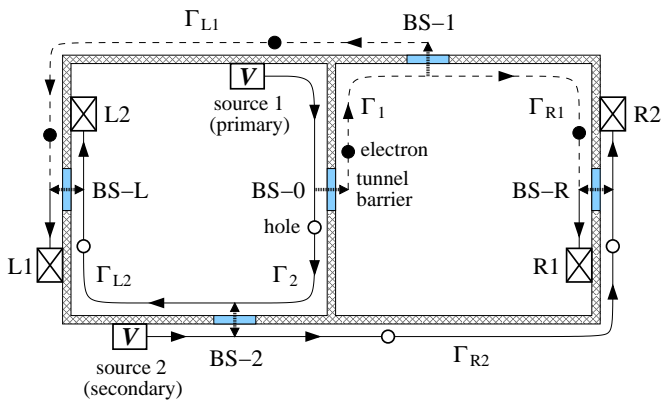


FIG. 2: Electronic analogue of the interferometer of Fig. 1 on a quantum Hall setup. Full (noiseless) electron streams—redefined vacuum (see text)—are represented by solid lines. Dashed lines correspond to empty electron channels.

ferometer. This keeps only that part of the two-photon state with one photon on each side of the interferometer: events in which two photons arrive in the same side are simply rejected. The postselected state corresponds to a coherent superposition of $|\Gamma_{L1}, \Gamma_{R2}\rangle$ and $|\Gamma_{R1}, \Gamma_{L2}\rangle$. The additional beam splitters BS-L and BS-R produce a local mixing required for detecting entanglement between left and right outgoing channels via the violation of Bell inequalities.¹⁴

An electronic analog of this photonic setup does not require an explicit rejection of double-click events on each side if, instead of measuring the times of detection—something difficult in electronic systems—, one measures zero-frequency current-noise cross correlations in the tunneling regime.^{11,15}

The purpose of the interferometer in Ref. 9 was to solve a fundamental deficiency in the Franson’s Bell experiment² based on energy-time and time-bin entanglement, identified by Aerts *et al.*¹⁶. Interestingly, the Franson’s interferometer (including its electronic analog) cannot be used to produce orbital entanglement, since the postselection in Franson’s scheme requires communication between the local parties and cannot be avoided by a local redefinition of the observables.

III. ELECTRONIC INTERFEROMETER

Figure 2 represents the electronic implementation of the interferometer of Fig. 1 on a quantum Hall system. The resulting device is feasible nowadays with modern experimental techniques.⁵ Though geometrically similar to that of Fig. 1, the electronic version has some singular features as a consequence of the fermionic nature of the carriers. Electrons propagate coherently along single-mode edge channels from sources 1 and 2 (subject to equal voltages V) to drains L1, L2, R1, and R2 (connected to earth). On their way, the electrons find a series of electrically controlled quantum point contacts

acting as beam splitters (BS- n , with $n = 0, 1, 2, L, R$). The BS-0 is set to be low transmitting (tunnel barrier). An electron propagating from *primary* source 1 can tunnel through BS-0 to the right side of the barrier, leaving a hole in the Fermi sea on the left side. So, BS-0 behaves as an electron-hole pair emitter (as discussed in Ref.¹⁰, with the difference that here we consider single—instead of double—channel propagation¹⁷). After emission, each member of the electron-hole pair splits independently into a pair of paths at BS-1 and BS-2, respectively, as discussed above. Path entanglement can be observed by zero-frequency current-noise cross correlations, which were shown^{11,15,18} to be equivalent to coincidence measurements in the tunneling regime. The *secondary* source 2 is not directly involved in the production of entanglement itself: its role is to eliminate the undesired current-noise correlations that otherwise would be generated at BS-2, masking the signal originated from the creation of electron-hole pairs at BS-0. Moreover, note that the resulting entanglement is not exactly between electrons on the one side and holes on the other side (in contrast to previous proposals^{10,11}), since both right and left propagating excitations can be either electronlike or holelike due to the combined action of BS-1 and BS-2. The BS-L and BS-R produce a controllable local mixing of right and left propagating channels, as discussed below.

IV. ENTANGLEMENT PRODUCTION

We start by introducing the uncorrelated state injected from sources $n = 1, 2$ as

$$|\Psi_{\text{in}}\rangle = \prod_{0 < \varepsilon < eV} a_1^\dagger(\varepsilon) a_2^\dagger(\varepsilon) |0\rangle, \quad (1)$$

where the operator $a_m^\dagger(\varepsilon)$ excites an electron towards BS-0 ($m = 1$) and BS-2 ($m = 2$) with energy ε on an energy window eV above the Fermi sea $|0\rangle$. Upon tunneling of electrons from source 1 through BS-0, the initial state (1) scatters as

$$|\Psi'\rangle = \prod_{\varepsilon} \left[t_0 b_1^\dagger(\varepsilon) + r_0 b_2^\dagger(\varepsilon) \right] a_2^\dagger(\varepsilon) |0\rangle, \quad (2)$$

where t_0 and r_0 are the scattering amplitudes at BS-0 ($T_0 = |t_0|^2 \ll R_0 = |r_0|^2$), and $b_n^\dagger(\varepsilon)$ excites a propagation mode from BS-0 toward BS- n ($n = 1, 2$). Expanding Eq. (2) up to first order in t_0 and using $b_2(\varepsilon) b_2^\dagger(\varepsilon) |0\rangle = |0\rangle$ (close to what is done in Ref.¹⁹), we find

$$|\Psi'\rangle \approx \left[1 - t_0 \int_0^{eV} d\varepsilon' b_2(\varepsilon') b_1^\dagger(\varepsilon') \right] \prod_{\varepsilon} b_2^\dagger(\varepsilon) a_2^\dagger(\varepsilon) |0\rangle. \quad (3)$$

The integral term in Eq. (3) corresponds to the emission (with probability $T_0 \ll 1$) of an electron-hole pair packet from BS-0, where the electron (b_1^\dagger) propagates to the right

and the hole (b_2) to the left (see Fig. 2). The hole appears as an excitation out of a full stream of particles toward BS-2 represented by $\prod_{\varepsilon} b_2^\dagger(\varepsilon)|0\rangle$. The electrons emitted from source 2 (a_2^\dagger) do not play any role in the generation of the electron-hole pair. Their relevance is proved only after scattering at BS-2, as we see next. Upon scattering at BS-1 and BS-2 (with amplitudes t_1, r_1 and t_2, r_2 , respectively), the intermediate state (3) evolves into

$$|\Psi_{\text{out}}\rangle = |\bar{0}\rangle + |\bar{\Psi}\rangle, \quad (4)$$

where

$$\begin{aligned} |\bar{\Psi}\rangle = & t_0 e^{i(\phi_1 - \phi_2)} \int_0^{eV} d\varepsilon' [t_1 t_2^* C_{L1}^\dagger(\varepsilon') C_{R2}(\varepsilon') \\ & - r_1 r_2^* C_{L2}(\varepsilon') C_{R1}^\dagger(\varepsilon') + t_1 r_2^* C_{L1}^\dagger(\varepsilon') C_{L2}(\varepsilon') \\ & + r_1 t_2^* C_{R1}^\dagger(\varepsilon') C_{R2}(\varepsilon')] |\bar{0}\rangle \end{aligned} \quad (5)$$

describes an electron-hole excitation out of a redefined vacuum $|\bar{0}\rangle = \prod_{\varepsilon}^{eV} C_{L2}^\dagger(\varepsilon) C_{R2}^\dagger(\varepsilon)|0\rangle$. Here, C_n^\dagger (C_n) creates an electron (hole) propagating towards terminal $n = L1, L2, R1$, or $R2$ (when BS-L and BS-R are *closed*) and ϕ_m is the phase acquired by an electron along path Γ_m with $m = 1, 2$. The redefined vacuum corresponds to a *noiseless* stream of electrons emitted from BS-2 toward terminals L2 and R2. This is only possible thanks to the introduction of the secondary source 2, which sets the net current through BS-2 to zero when BS-0 is closed. Otherwise, electrons from primary source 1 alone would be scattered at BS-2 as correlated noisy currents, masking the signatures of the electron-hole emission at BS-0.

Having a look at $|\bar{\Psi}\rangle$ in Eq. (5), and leaving aside the specific features of electrons, we notice that the electron-hole pair emitted from BS-0 suffers from an evolution wholly analogous to the one described in Ref.⁹ for photon pairs (as discussed above).

The first two terms within brackets in Eq. (5) show a coherent superposition of an electron and a hole traveling, alternately, toward opposite sides of the interferometer along different paths. This is the part of the state we are interested in, corresponding to a pair of ‘‘orbital’’ qubits,²⁰ which can be entangled depending on the relative weights given by the scattering amplitudes at BS-1 and BS-2. The entanglement of a normalized two-qubit pure state $|\Psi\rangle$ can be quantified by the concurrence $0 \leq \mathcal{C}(\Psi) = |\langle \Psi | \tilde{\Psi} \rangle| \leq 1$,²¹ where $|\tilde{\Psi}\rangle = \sigma_y \otimes \sigma_y |\Psi^*\rangle$ is the time reverse of $|\Psi\rangle$ (with σ_y the second Pauli matrix), $\mathcal{C}(\Psi) = 0$ for separable states (no entanglement), and $\mathcal{C}(\Psi) = 1$ for Bell states (maximal entanglement). Applying this to the first two terms in Eq. (5), after normalization, we obtain

$$\mathcal{C} = 2 \frac{\sqrt{T_1 T_2 R_1 R_2}}{T_1 T_2 + R_1 R_2}, \quad (6)$$

where T_1 (R_1) and T_2 (R_2) are the transmission (reflection) probabilities at BS-1 and BS-2, respectively. Maximal entanglement is achieved whenever $T_1 T_2 = R_1 R_2$.

The last two terms within brackets in Eq. (5), instead, correspond to a particle and a hole traveling both either to the right or to the left side of the interferometer. This part of the state (subject to occupation-number entanglement only) shall be filtered out during measurement.

V. ENTANGLEMENT DETECTION

At this point, we can drop out of the electron-hole picture introduced above, which was only a convenient frame for revealing the process of entanglement production. From now on we work within the standard electron picture, which simplifies the description of the detection procedure. In the tunneling regime, entanglement can be detected via the violation of Bell-like inequalities¹⁴ constructed upon the measurement of zero-frequency current-noise cross correlations defined as

$$S_{ij} = \lim_{\mathcal{T} \rightarrow \infty} \frac{h\nu}{\mathcal{T}^2} \int_0^{\mathcal{T}} dt_1 dt_2 \langle \delta I_{Li}(t_1) \delta I_{Rj}(t_2) \rangle. \quad (7)$$

This quantity correlates the time-dependent current fluctuations δI_{Li} at the left terminals ($i = 1, 2$) with the fluctuations δI_{Rj} at the right terminals ($j = 1, 2$), where \mathcal{T} is the measurement time and ν is the density of states [a discrete spectrum is considered to ensure a proper regularization of the current-noise correlations (see Ref. 7)]. The last two terms in Eq. (5) do not contribute to S_{ij} , since this is a two-particle observable demanding the presence of one particle on each side of the interferometer for detection. Thanks to this, only the first two terms in Eq. (5) are postselected. At low temperatures ($kT \ll eV$), the cross correlator reads²² as

$$S_{ij} = -e^3 V / h | (t_L t_R^\dagger)_{ij} |^2, \quad (8)$$

where the 2×2 matrices t_L and t_R contain the scattering amplitudes from sources 1 and 2 to terminals L1 and L2 the first one, and to R1 and R2 the second one. They satisfy $t_L^\dagger t_L + t_R^\dagger t_R = \mathbb{1}$ due to unitarity of the scattering matrix. The S_{ij} turns out to be proportional to the tunneling probability T_0 (i.e., $S_{ij} \propto T_0$), meaning that any correlation signal is due to the emission of electron-hole pairs from BS-0 alone. This is only possible thanks to the presence of secondary source 2: otherwise, S_{ij} would be finite even for $T_0 = 0$, due to the undesired correlated noise generated at BS-2. So defined, the correlator S_{ij} is proportional to the probability of joint detection of particles in terminals i and j (an electron on one side and a hole on the other).^{11,15,18} The presence of finite reference currents at both sides of the interferometer (redefined vacuum $|\bar{0}\rangle$) does not change this fact. This is because the current-noise correlators are independent of the noiseless reference currents (an alternative formulation based on pure tunneling currents can be used with identical results). A Bell inequality can be constructed

upon S_{ij} by defining the correlation function

$$E = \frac{S_{11} + S_{22} - S_{12} - S_{21}}{S_{11} + S_{22} + S_{12} + S_{21}} = \frac{\text{tr} \left(\sigma_z t_L^\dagger t_R^\dagger \sigma_z t_R t_L \right)}{\text{tr} \left(t_L^\dagger t_L t_R^\dagger t_R \right)}, \quad (9)$$

where σ_z is the third Pauli matrix. The correlator E is explored by introducing an additional local mixing of left and right outgoing channels. This is implemented through the beam splitters BS-L and BS-R, as shown in Fig. 2, from which the transmission matrices transform as $t_L \rightarrow U_L t_L$ and $t_R \rightarrow U_R t_R$, where U_L and U_R are the corresponding 2×2 unitary scattering matrices.²³ Hence, the correlator E transforms as

$$E(U_L, U_R) = \frac{\text{tr} \left(U_L^\dagger \sigma_z U_L t_L^\dagger t_R^\dagger U_R^\dagger \sigma_z U_R t_R t_L \right)}{\text{tr} \left(t_L^\dagger t_L t_R^\dagger t_R \right)}, \quad (10)$$

from which the Bell-Clauser-Horne-Shimony-Holt (CHSH) operator is defined as¹⁴

$$\mathcal{E} = E(U_L, U_R) + E(U_L', U_R) + E(U_L, U_R') - E(U_L', U_R'). \quad (11)$$

The studied state is entangled if the Bell-CHSH operator satisfies $|\mathcal{E}| > 2$ for some configurations of matrices $\{U_L, U_R, U_L', U_R'\}$. Following Refs. 10 and 24, we find that the maximum possible value for the Bell-CHSH operator (11) reads as

$$\mathcal{E}_{\max} = 2 \sqrt{1 + \frac{4(1 - \lambda_+)(1 - \lambda_-)\lambda_+\lambda_-}{(\lambda_+ + \lambda_- - \lambda_+^2 - \lambda_-^2)^2}}, \quad (12)$$

where $\lambda_+ = 1 - T_0 T_1 T_2$ and $\lambda_- = T_0 R_1 R_2$ are the eigenvalues of the matrix product $t_R^\dagger t_R$ up to first order in the tunneling probability T_0 . We notice that Eq. (12) reduces to $\mathcal{E}_{\max} = 2\sqrt{1 + \mathcal{C}^2}$ with \mathcal{C} the concurrence of Eq. (6). This is an expected relation for a pair of entangled qubits,^{10,25} which guarantees the accuracy of our approach. Its meaning is straightforward in our case: whenever there is orbital entanglement in the emitted state $|\bar{\Psi}\rangle$ of Eq. (5) ($\mathcal{C} > 0$), there is a violation of the Bell-CHSH inequality $|\mathcal{E}| \leq 2$.

VI. CONCLUSIONS

The production and detection of entanglement are still a major challenge for quantum electronics. Here we have described a source of orbital entanglement in an electron-hole quantum Hall systems. We have discussed how to use it to prepare entangled states and characterize entanglement and quantum nonlocality. A fundamental feature is that the scheme is simpler than previous proposals and seems feasible with present technology, so we expect that it can stimulate further experimental developments in electronic quantum information.

Acknowledgments

We acknowledge support from the Ramón y Cajal program, from the Spanish Ministry of Science and Innovation's Project No. FIS2008-05596, and from the Junta de Andalucía's Excellence Projects No. P06-FQM-2243 and No. P07-FQM-3037.

* Electronic address: frustaglia@us.es

† Electronic address: adan@us.es

¹ P.G. Kwiat, K. Mattle, H. Weinfurter, A. Zeilinger, A.V. Sergienko, and Y. H. Shih, Phys. Rev. Lett. **75**, 4337 (1995).

² J.D. Franson, Phys. Rev. Lett. **62**, 2205 (1989).

³ Y. Ji, Y. Chung, D. Sprinzak, M. Heiblum, D. Mahalu, and H. Shtrikman, Nature (London) **422**, 415 (2003).

⁴ M. Henny, S. Oberholzer, C. Strunk, T. Heinzel, K. Ensslin, M. Holland, and C. Schönberger; Science **284**, 296 (1999); W.D. Oliver, J. Kim, R.C. Liu, and Y. Yamamoto, *ibid.* **284**, 299 (1999); S. Oberholzer, M. Henny, C. Strunk, C. Schönberger, T. Heinzel, K. Ensslin, and M. Holland, Physica (Amsterdam) **6E**, 314 (2000); H. Kiesel, A. Renz, and F. Hasselbach, Nature (London) **418**, 392 (2002).

⁵ I. Neder, N. Ofek, Y. Chung, M. Heiblum, D. Mahalu, and V. Umansky, Nature (London) **448**, 333 (2007).

⁶ R. Hanbury Brown and R.Q. Twiss, Nature (London) **177**, 27 (1956).

⁷ V. Giovannetti, D. Frustaglia, F. Taddei, and R. Fazio, Phys. Rev. B **74**, 115315 (2006).

⁸ C.K. Hong, Z.Y. Ou, and L. Mandel, Phys. Rev. Lett. **59**, 2044 (1987).

⁹ A. Cabello, A. Rossi, G. Vallone, F. De Martini, and P.

Mataloni, Phys. Rev. Lett. **102**, 040401 (2009).

¹⁰ C.W.J. Beenakker, C. Emary, M. Kindermann, and J.L. van Velsen, Phys. Rev. Lett. **91**, 147901 (2003).

¹¹ P. Samuelsson, E.V. Sukhorukov, and M. Büttiker, Phys. Rev. Lett. **92**, 026805 (2004).

¹² P. Samuelsson and M. Büttiker, Phys. Rev. B **71**, 245317 (2005).

¹³ H.M. Wiseman and J.A. Vaccaro, Phys. Rev. Lett. **91**, 097902 (2003); N. Schuch, F. Verstraete, and J.I. Cirac, *ibid.* **92**, 087904 (2004); V. Giovannetti, D. Frustaglia, F. Taddei, and R. Fazio, Phys. Rev. B **75**, 241305(R) (2007).

¹⁴ J.S. Bell, Physics (Long Island City, N.Y.) **1**, 195 (1964); J.F. Clauser, M.A. Horne, A. Shimony, and R.A. Holt, Phys. Rev. Lett. **23**, 880 (1969).

¹⁵ P. Samuelsson, E.V. Sukhorukov, and M. Büttiker, Phys. Rev. Lett. **91**, 157002 (2003).

¹⁶ S. Aerts, P.G. Kwiat, J.-Å. Larsson, and M. Żukowski, Phys. Rev. Lett. **83**, 2872 (1999); **86**, 1909 (2001).

¹⁷ For the sake of simplicity, we consider the spinless case only. Spin-degenerate channels can be introduced without any significant consequence on orbital entanglement due to separability of spin and orbital degrees of freedom.

¹⁸ C.W.J. Beenakker, in *Quantum Computers, Algorithms and Chaos*, Proceedings of the International School of

Physics “Enrico Fermi”, Varenna, 2005 (IOS Press, Amsterdam, 2006).

¹⁹ P. Samuelsson, E.V. Sukhorukov, and M. Büttiker, N. J. Phys. **7**, 176 (2005).

²⁰ We identify the two levels of each qubit with the pair of outgoing channels at each side of the interferometer (along which only one particle- electron or hole- propagates). Defining the *upper*-state of each qubit as the electron excitation, $|1\rangle = C_{(L,R)1}^{\dagger}|\bar{0}\rangle$, and the *lower*-state as the hole one, $|0\rangle = C_{(L,R)2}|\bar{0}\rangle$, the first two terms in Eq. (5) read as $t_1 t_2^* |10\rangle - r_1 r_2^* |01\rangle$.

²¹ W.K. Wootters, Phys. Rev. Lett. **80**, 2245 (1998).

²² M. Büttiker, Phys. Rev. Lett. **65**, 2901 (1990).

²³ The U_L and U_R mixing matrices can absorb the kinetic/magnetic phases acquired by the electrons (and holes) along their way from BS-1 and BS-2 to drains, so we do not need to consider them explicitly. Notice that the mixing can be performed either by controlling the transmission amplitude of BS-L and BS-R, by modifying the Aharonov-Bohm flux through the interferometer, or by introducing local electric gates that modify the length of selected paths towards the left and/or right side of the interferometer.

²⁴ S. Popescu and D. Rohrlich, Phys. Lett. A **166**, 293 (1992).

²⁵ N. Gisin, Phys. Lett. A **154**, 201 (1991).